Journal of Biomolecular NMR, 10 (1997) 129–142
KLUWER/ESCOM
© 1997 *Kluwer Academic Publishers. Printed in The Netherlands.*

J-Bio NMR 457

Protein ϕ and ψ dihedral restraints determined from multidimensional hypersurface correlations of backbone chemical shifts and their use in the determination of protein tertiary structures

Richard D. Beger and Philip H. Bolton*

Department of Chemistry, Wesleyan University, Middletown, CT 06459, U.S.A.

Received 20 December 1996
Accepted 5 April 1997

Keywords: Protein structure; Chemical shifts; Dihedral restraints

Summary

The chemical shifts of the backbone atoms of proteins can be used to obtain restraints that can be incorporated into structure determination methods. Each chemical shift can be used to define a restraint and these restraints can be simultaneously used to define the local, secondary structure features. The global fold can be determined by a combined use of the chemical shift based restraints along with the long-range information present in the NOEs of partially deuterated proteins or the amide–amide NOEs but not from such limited NOE data sets alone. This approach has been demonstrated to be capable of determining the overall folding pattern of four proteins. This suggests that solution-state NMR methods can be extended to the structure determination of larger proteins by using the information present in the chemical shifts of the backbone atoms along with the data that can be obtained on a small number of labeled forms.

Introduction

The chemical shifts of proteins and other molecules have been used for quite some time to obtain qualitative structural information. The chemical shifts of the amide protons and amide nitrogens of a protein typically offer considerable hints about the amount of β-structure present. For example, the examination of the chemical shifts of the amide nitrogens and protons of a protein can usually allow an experienced spectroscopist to make a fairly reliable estimation of the amount of β-structure present in the protein. The conversion of chemical shift information into quantifiable structural information has not yet been completely made.

It was clear to us, as to others before us, that the chemical shift of any one site does not contain enough information to tightly define a dihedral angle as there are several contributing factors to the chemical shifts. However, the simultaneous use of the chemical shifts of many atom sites might allow an accurate prediction of the actual dihedral angles. Empirical correlations between the chemical shift of a backbone atom and a dihedral angle can be based on existing experimental data sets. As shown below, the simultaneous use of the independent correlations of five backbone atoms can be used to generate a probability map for the dihedral angles of that amino acid and these probability maps can be incorporated into structure determination methods of proteins both large and small.

Chemical shifts have been used as qualitative probes of the α- and β-structural features of proteins (Sternlicht and Wilson, 1967; Tigelaar and Flygare, 1972; Clayden and Williams, 1982; Spera and Bax, 1991). For example, the resonances of amide proteins and α-protons in β-strands typically appear downfield of those of other structural elements. The $^{13}C^{\alpha}$ and $^{13}C^{\beta}$ chemical shifts have been used as prime information in protein secondary structure determination (Kuszewski et al., 1995; Laws et al., 1995; Le et al., 1995). Protein structures have been refined using the information in the chemical shifts of the α- and β-carbons (Kuszewski et al., 1995; Pearson et al., 1995). Theoretical calculations have indicated that the ^{1}H, ^{13}C,

*To whom correspondence should be addressed.

TABLE 1
PROTEINS AND BACKBONE ATOMS USED IN THE DETERMINATION OF NMR CHEMICAL SHIFT AVERAGES VERSUS THEIR ϕ AND ψ DIHEDRAL ANGLES

Protein	PDB	X-ray coord. (+)	Labeling	^{15}N amide	H^N	H^α	C^α	C^β	CO
Antibody V_L domain (Constantine et al., 1992,1993)	1maj		C, N	99	99	105	63	59	–
Apokedarcidin (Constantine et al., 1994)	1akp		C, N	108	108	111	111	95	–
Calbindin D9k (Skelton et al., 1990,1992)	2bca		N	68	68	72	–	–	–
Calmodulin (Ikura et al., 1990,1992)	2bbm		C, N	143	143	146	146	–	146
Chemotaxis Y (Moy et al., 1994)	1cey		C, N	114	114	124	123	113	–
Cro-repressor (Matsuo et al., 1995)	1cop		C, N	62	62	64	64	59	–
Cyclophilin (Clubb et al., 1993,1994)	1clh		C, N	149	149	158	158	–	161
ETS domain (Donaldson et al., 1994)	1etc		C, N	95	95	100	101	94	99
Ferredoxin (Oh and Markley, 1990; Rypniewski et al., 1991)	1fxa	+	C, N	74	74	78	78	74	42
FK506 (Duyne et al., 1991; Xu et al., 1993)	1fkf	+	C, N	97	97	105	105	–	92
GATA-1 (Clore et al., 1994)	1gat		C, N	55	55	58	58	54	–
Glucocortoid (Berglund et al., 1992; Baumann et al., 1993)	1gdc		N	64	64	–	–	–	–
Growth factor (Erikson et al., 1991; Powers, 1996)	4fgf	+	C, N	115	115	120	122	109	115
Heat shock protein (Vuister et al., 1994)	1hks		C, N	95	95	103	103	97	95
High pot. iron-sulfur (Banci et al., 1994; Bertini et al., 1994)	1pih		N	57	57	58	–	–	–
Histone (Cerf et al., 1994)	1ghc		N	72	72	73	–	–	–
HU (Vis et al., 1994,1995)	1hue		C, N	84	84	88	88	79	88
Interferon γ (Grzesiek et al., 1992; S.E. Ealick (1996) personal communication)	itf	+	C, N	–	–	–	–	–	114
Interleukin-1 (Stockman et al., 1992,1994)	1irp		N	127	127	–	–	–	–
Interleukin-1β (Clore et al., 1991)	6i1b		N	143	143	149	–	–	–
Interleukin-4 (Powers et al., 1992,1993)	1itm		C, N	121	121	127	127	123	127
Lysozyme (Rose et al., 1988; McIntosh et al., 1990)	1lyd	+	N	159	159	155	–	–	–
Macrophage inhibitory protein (Garrett et al., 1994; Lodi et al., 1994)	1hum		C, N	59	59	65	65	65	–
MutT enzyme (Abeygunawardana et al., 1993,1995)	mut		C, N	114	114	123	123	113	126
Myoglobin (Ösapay et al., 1994; Theirault et al., 1994)	1myf		N	142	142	143	–	–	–
Ner (Gronenborn et al., 1989)	1neq		N	63	63	63	–	–	–
NTRC receiver (Volkman et al., 1995)	1ntr		C, N	99	99	116	115	108	–
Oct-1 (Cox et al., 1993; Strzelecka et al., 1995)	1oct	+	N	66	66	68	–	–	–
c-Myb oncoprotein (Jamin et al., 1993)	1mse		C, N	87	87	91	91	–	–
p53 oligomerization (Clore et al., 1995)	1olg		C, N	37	37	36	36	35	–
p53 transforming (Lee et al., 1994b)	1pes		C, N	29	29	29	29	28	29
Papillomavirus E2 (Liang et al., 1996)	pe2		C, N	75	75	78	78	74	–
Phosphotransferase (Van Nuland et al., 1992,1995)	1hdn		C, N	80	80	82	82	–	–
Photosystem I subunit (Falzone et al., 1994a,b)	1pse		N	66	66	66	–	–	–
Plasminogen activator (Hansen et al., 1994)	1urk		C, N	111	111	121	112	98	–
Profilin (Metzler et al., 1993)	1pfl		C, N	132	132	137	137	121	–
Profilin (Vinson et al., 1993)	2prf		C, N	119	119	122	122	107	–
Protein spore Coat (Bagby et al., 1994a,b)	1prr		C, N	148	148	163	163	–	–
Recoverin (Flaherty et al., 1993; Ames et al., 1994)	1rec	+	C, N	175	175	181	181	163	176
Shc SH2 domain (S.W. Fesik (1996) personal communication)	seg		C, N	97	97	104	104	97	103
Sex-lethal (Lee et al., 1994a)	1sxl		C, N	86	86	85	85	75	–
Staph nuclease (Loll and Lattman, 1989; Hynes and Fox, 1991; Wang et al., 1992)	1srt	+	C, N	116	116	–	105	–	–
Stromelysin (Gooley et al., 1993,1994)	2str		C, N	128	128	134	134	–	145
Thioredoxin (Forman-Kay et al., 1990,1991)	3trx		N	96	96	103	–	–	–
Topoisomerase I (Yu et al., 1995)	1yua		C, N	103	103	113	113	106	–
Trans. growth factor (Archer et al., 1993; Schlunegger and Gruetter, 1993)	1tfg	+	N	58	58	59	–	–	–
Trp repressor (Lawson et al., 1988; Borden et al., 1992)	1wrp	+	C, N	94	94	94	102	97	–
Uracil glycosylase inhibitor (Balasubramanian et al., 1995; Beger et al., 1995)	ugi		C, N	74	74	67	20	–	–
Villin 14T (Markus et al., 1994; G. Wagner (1996) personal communication)	1vil		C, N	118	118	121	121	88	122

and ^{15}N chemical shifts of proteins are primarily dependent on the local environment. These calculations have demonstrated considerable ability to predict ^{1}H, ^{13}C, and ^{15}N chemical shifts from protein structures (Wüthrich, 1986; Szilagyi and Jardetzky, 1989; Pastore and Saudek, 1990; Wishart et al., 1992; Wishart and Sykes, 1994).

The approach used here is to empirically correlate the observed chemical shifts of the backbone atoms with the observed dihedral angles. This was done for all the five backbone atoms as well as for all the five sites simultaneously. The simultaneous use of all five chemical shifts allows the ϕ and ψ dihedral angles to be well defined. This allows the local structural features to be determined by chemical shifts.

Since the chemical shifts primarily report on the local, secondary structure elements, at least one additional type of structural information is needed for tertiary structure determination. The long-range information in the amide–amide NOEs can be sufficient. Amide–amide NOEs can be selectively observed with suppression of spin diffusion even for larger proteins with the use of only ^{15}N labeling (Vincent et al., 1996). Long-range NOEs involving other protons can be observed with effective suppression of spin diffusion by the use of partially deuterated proteins (Gardner et al., 1997). The combination of the information present in chemical shifts along with limited, long-range NOE information is shown below to be sufficient for protein structure determination and the needed information can be obtained on large proteins. The chemical shift information primarily defines the local secondary structure features and the long-range NOEs primarily give the overall folding pattern.

Methods

A database for correlating chemical shifts and dihedral angles was constructed using the results on 49 proteins that have had their structures and chemical shifts determined. The relevant properties of these proteins are listed in Table 1. This database was used to obtain the empirical correlations between the chemical shifts of amide ^{15}N, $^{13}C^{\alpha}$ and $^{13}C^{\beta}$, amide proton and $^{1}H^{\alpha}$ with the ϕ and ψ dihedral angles. Correlation plots of the chemical shifts of each of these five backbone atoms, of each type of amino acid, versus the ϕ and ψ dihedral angles were constructed. The ϕ,ψ surface was divided into 216 bins, with 180 bins of 20° by 20° and 36 bins of 40° by 40°. Larger bins were used in the regions with the fewest occupants.

The four bins around $\phi = -60°$, $\psi = -40°$ were used to obtain an average 'intrinsic' α-helical chemical shift for each amino acid and the four bins around $\phi = -120°$, $\psi = 120°$ were averaged to produce an 'intrinsic' β-sheet chem-

TABLE 2
AVERAGE CHEMICAL SHIFT SCORES FOR ALL 20 AMINO ACIDS AND THE TEMPLATE AROUND THE FOUR BINS AROUND $\phi = -60°$ AND $\psi = -40°$ THAT DETERMINED THE AVERAGE INTRINSIC CHEMICAL SHIFT AVERAGE FOR α-HELICES, AND THE FOUR BINS AROUND $\phi = -120°$ AND $\psi = 120°$ THAT DETERMINED THE INTRINSIC CHEMICAL SHIFT AVERAGE FOR β-SHEETS

Amino acid	Amide N		Amide H		$^{1}H^{\alpha}$		$^{13}C^{\alpha}$		$^{13}C^{\beta}$		^{13}CO	
	α	β	α	β	α	β	α	β	α	β	α	β
Ala	122.0 (141)	123.5 (16)	8.1 (141)	8.3 (16)	4.04 (132)	4.86 (13)	54.4 (92)	50.3 (10)	18.2 (63)	20.8 (8)	178.7 (47)	175.1 (4)
Arg	119.9 (83)	122.9 (23)	8.2 (83)	8.6 (23)	3.91 (78)	4.83 (21)	59.0 (61)	54.0 (18)	29.9 (51)	33.5 (12)	178.1 (29)	174.5 (14)
Asn	117.3 (43)	118.0 (10)	8.3 (43)	8.3 (10)	4.42 (42)	5.07 (9)	55.2 (27)	52.9 (6)	37.9 (20)	40.2 (5)	176.8 (11)	174.6 (2)
Asp	119.2 (65)	124.1 (7)	8.3 (65)	8.6 (7)	4.43 (65)	5.20 (5)	56.5 (44)	52.6 (4)	39.6 (34)	42.1 (3)	177.6 (25)	172.6 (1)
Cys	120.4 (11)	122.5 (11)	8.7 (11)	9.2 (11)	4.19 (7)	5.10 (10)	59.5 (4)	55.4 (4)	36.9 (3)	43.1 (4)	175.2 (2)	
Gln	117.4 (64)	122.0 (28)	8.2 (64)	8.4 (28)	4.00 (60)	5.05 (24)	58.3 (40)	53.9 (18)	28.0 (28)	30.9 (9)	178.0 (22)	175.0 (7)
Gly	106.7 (37)	110.6 (6)	8.3 (146)	8.8 (6)	3.73 (34)	4.47 (6)	46.8 (20)	44.6 (3)				
Glu	119.4 (146)	122.9 (22)	8.3 (146)	8.7 (22)	3.99 (141)	4.91 (19)	59.0 (101)	53.8 (16)	28.9 (78)	32.0 (12)	177.9 (64)	174.8 (8)
His	119.2 (26)	120.4 (10)	8.1 (26)	8.7 (10)	4.25 (24)	5.22 (8)	58.6 (18)	53.3 (9)	29.5 (12)	31.8 (7)	177.0 (12)	174.2 (4)
Ile	119.8 (72)	123.6 (36)	8.1 (72)	8.8 (36)	3.69 (72)	4.69 (31)	63.8 (51)	58.9 (24)	36.8 (35)	39.7 (20)	177.3 (35)	174.1 (11)
Leu	120.2 (147)	123.8 (45)	8.1 (147)	8.7 (45)	4.03 (142)	4.82 (39)	57.3 (95)	53.3 (30)	41.2 (67)	43.9 (23)	178.0 (47)	175.9 (16)
Lys	119.5(107)	121.7 (26)	8.1 (107)	8.5 (26)	4.00 (100)	4.84 (23)	58.5 (62)	54.1 (19)	31.8 (47)	35.0 (14)	178.0 (42)	175.5 (12)
Met	118.3 (29)	120.7 (8)	8.1 (29)	8.3 (8)	4.25 (25)	4.82 (6)	57.4 (20)	54.5 (6)	31.8 (12)	35.6 (6)	178.2 (13)	174.9 (5)
Pro					4.26 (30)		64.6 (27)		31.5 (20)		178.0 (14)	
Phe	120.6 (16)	121.3 (13)	8.4 (16)	8.7 (13)	4.15 (47)	5.14 (25)	60.8 (31)	56.2 (21)	38.5 (20)	41.6 (14)	176.8 (26)	174.5 (11)
Ser	116.6 (46)	116.2 (19)	8.2 (46)	8.6 (19)	4.16 (43)	5.18 (19)	61.0 (30)	56.5 (16)	62.1 (20)	65.1 (14)	175.7 (21)	173.1 (6)
Thr	115.0 (55)	115.4 (37)	8.1 (55)	8.2 (37)	3.98 (55)	4.93 (30)	65.3 (39)	60.4 (30)	68.0 (32)	70.0 (24)	175.9 (23)	173.9 (10)
Trp	119.9 (18)	122.3 (4)	8.2 (18)	8.5 (4)	4.28 (55)	5.08 (3)	60.1 (13)	55.0 (2)	28.5 (11)	31.7 (2)	177.5 (7)	174.1 (2)
Tyr	119.5 (31)	121.3 (16)	8.2 (31)	8.6 (16)	4.19 (29)	4.95 (14)	60.7 (25)	56.4 (9)	37.8 (20)	41.5 (7)	176.7 (16)	175.8 (8)
Val	120.0 (76)	121.3 (66)	8.0 (76)	8.6 (66)	3.48 (74)	4.78 (60)	65.6 (53)	59.9 (49)	31.2 (35)	34.2 (39)	177.4 (30)	174.1 (14)
Temp	119.4 (957)	122.1 (331)	8.2 (957)	8.6 (331)	4.02 (919)	4.89 (287)	59.3 (647)	55.9 (248)	33.8 (474)	37.1 (175)	177.6 (374)	174.8 (97)

Next to the chemical shift scores the numbers in parentheses represent the number of chemical shifts used from the four bins used to determine the α-helix and β-sheet average intrinsic chemical shift score. In the last row, Temp stands for the 14 amino acid template.

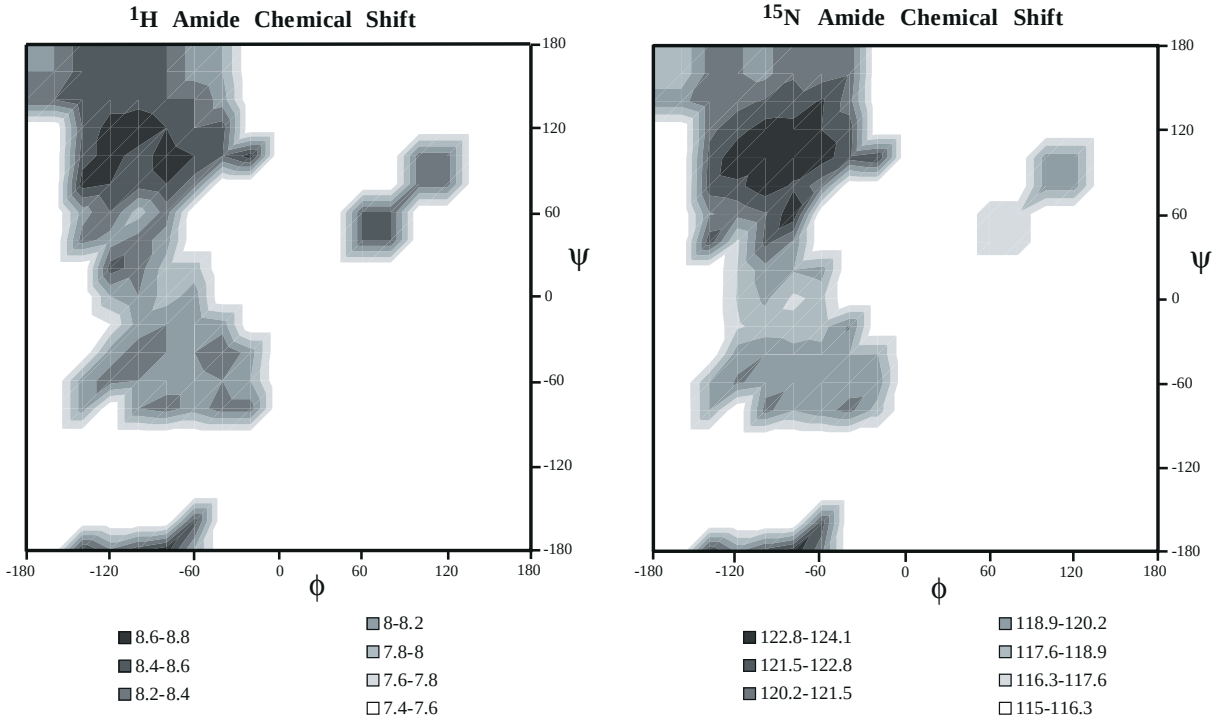

Fig. 1. Average of the ^{1}H amide and ^{15}N amide chemical shifts of all the amino acids, except for the cysteine, proline, glycine, serine, alanine, and threonine residues, versus their ϕ and ψ dihedral angles.

ical shift as indicated in Table 2. The α-helical chemical shift profile of each individual amino acid was defined by adding the deviation between the intrinsic α-helix chemical shift of the 14 amino acid template and the intrinsic α-helical chemical shift of the particular amino acid to all the bins of the α-helical part of the template. The β-sheet chemical shift profile of each individual amino acid was defined in the same manner.

To improve the statistics, the results on all the amino acids, except for cysteine, proline, glycine, serine, alanine, and threonine, were combined to produce the correlation maps for the chemical shifts of the backbone atoms. The chemical shift templates of each of the five atoms were then refined by removing all bins that did not contain at least five ^{15}N, $^{1}H^{N}$, $^{1}H^{\alpha}$, $^{13}C^{\alpha}$ and $^{13}C^{\beta}$ chemical shifts. The resulting chemical shift templates corresponded to a region in the ϕ,ψ surface that contained more than 96% of all the available chemical shifts. These refined chemical shift templates were used to determine the chemical shift dihedral restraints for all the amino acids, except for glycine and proline, during the structure calculations.

Alanine was excluded from the construction of the template because of the large deviation between the $^{13}C^{\beta}$ chemical shift of the 14 amino acid template and that of alanine as indicated by the results in Table 2. Serine and threonine were also excluded from the construction of the template because of the large deviations between the averaged intrinsic ^{15}N, $^{13}C^{\alpha}$, and $^{13}C^{\beta}$ chemical shifts of the 14 amino acid template and those of serine and threonine as indicated by the results in Table 2. The ^{15}N and $^{13}C^{\beta}$ chemical shifts of threonine are dependent on the dihedral angle χ_1 (de Dios and Oldfield, 1994; Le and Oldfield, 1994). Cysteine was not included in the construction of the template because there were too few cysteine residues in the database to assess the quality of the correlations. Glycine and proline were removed from their templates because their backbones are different from those of the other 14 amino acids.

The correlation plots for each amino acid type template were separated into three regions: an α-helical region, $-140° < \phi < -20°$, $-100° < \psi < -20°$; a β-sheet region, $-180° < \phi < -40°$, $80° < \psi < 180°$; and all other bins. The chemical shift profiles of the individual amino acids were put on a common scale by adding the difference between the intrinsic α-helix chemical shift of the 14 amino acid template and the intrinsic α-helix chemical shift of the particular amino acid to all the chemical shifts of the particular amino acid in the α-helical region. The same procedure was carried out for the β-regions. Correlation plots of the average chemical shift versus the ϕ and ψ dihedral angles for the 14 amino acid template are, for each of the backbone atoms ^{15}N, $^{1}H^{N}$, $^{1}H^{\alpha}$, $^{13}C^{\alpha}$, $^{13}C^{\beta}$ and ^{13}CO, as shown in Figs. 1–3. Correlation plots were constructed for all the amino acids, except for proline and glycine.

The amide ^{15}N and proton chemical shifts have been used to qualitatively determine secondary structural features. Downfield shifts of amide ^{15}N and amide ^{1}H are

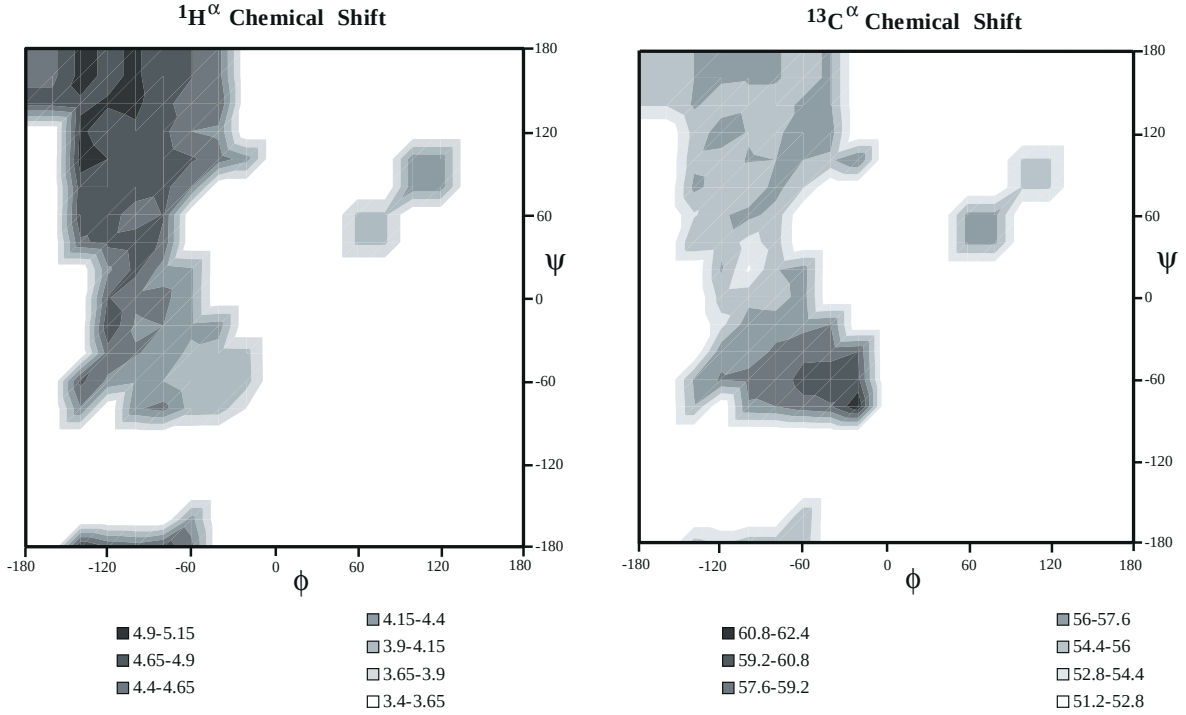

Fig. 2. Average of the $^{1}H^{\alpha}$ and $^{13}C^{\alpha}$ chemical shift templates of all the amino acids, except for the cysteine, proline, glycine, serine, alanine, and threonine residues, versus their ϕ and ψ dihedral angles.

indicators of the presence of β-structural features. The analysis of the 49 proteins puts these notions on a stronger statistical footing, as shown in Fig. 1.

The results in Fig. 2 also support the sort of correlations commonly made between structural elements and chemical shifts. The results in Fig. 2 show that the most

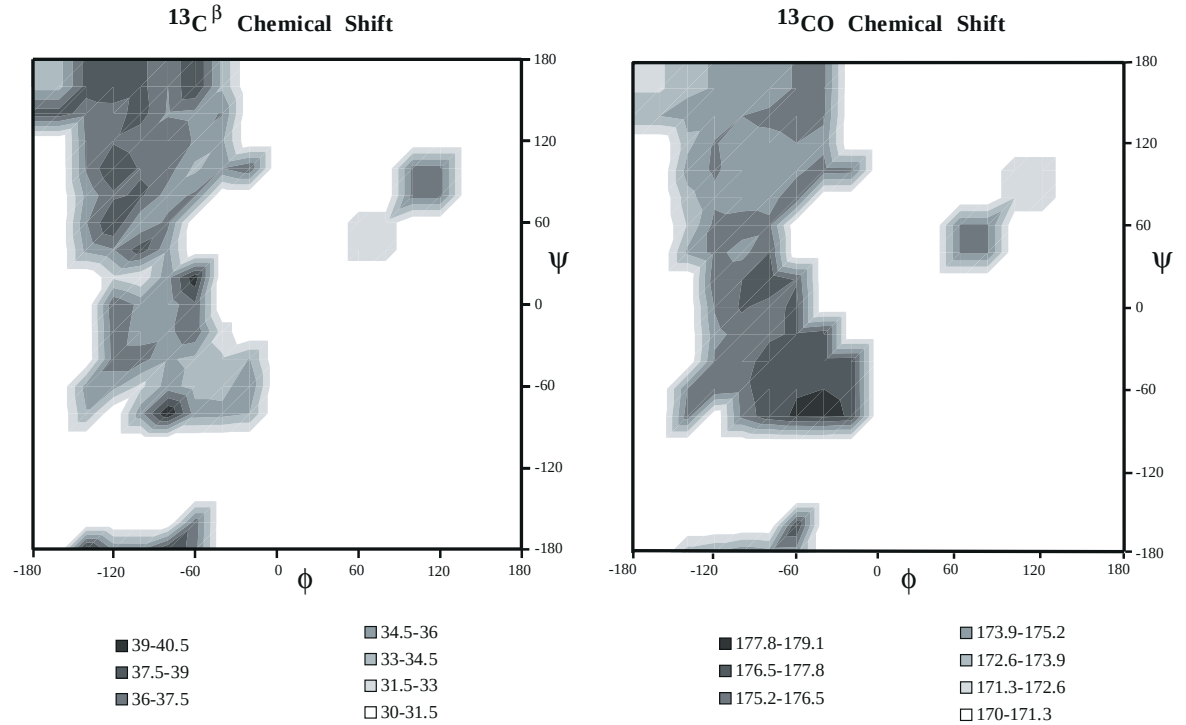

Fig. 3. Average of the $^{13}C^{\beta}$ and ^{13}CO chemical shift templates of all the amino acids, except for the cysteine, proline, glycine, serine, alanine, and threonine residues, versus their ϕ and ψ dihedral angles.

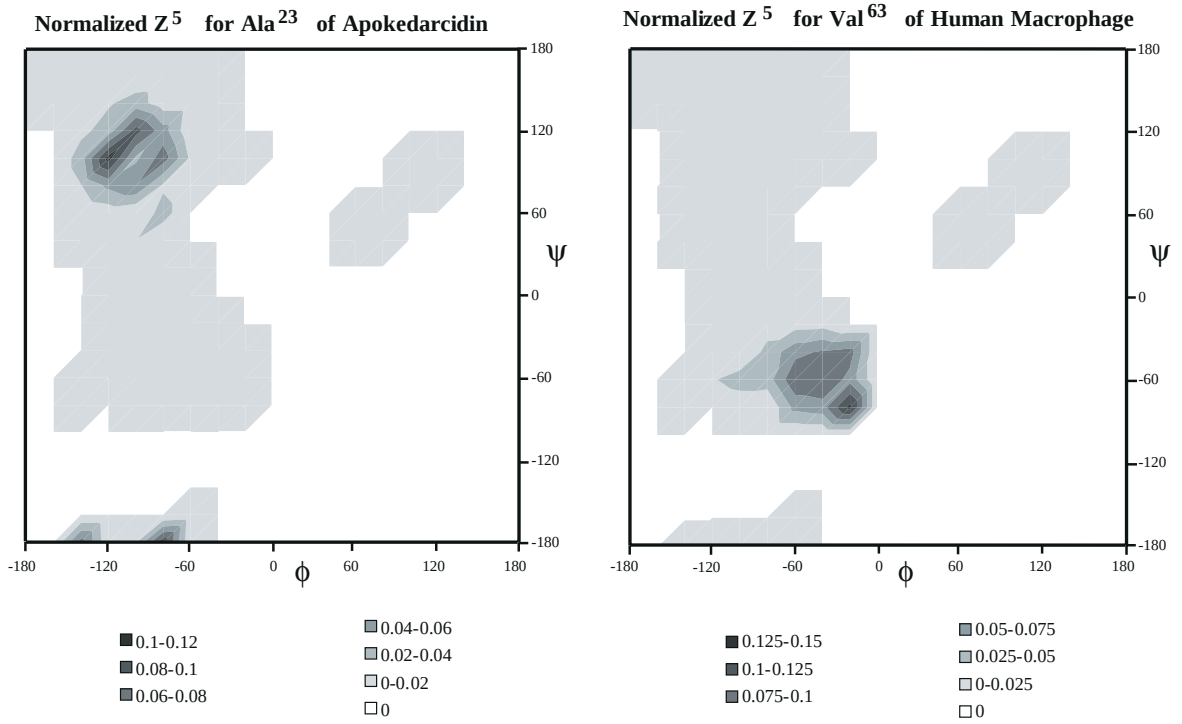

Fig. 4. (Left) Normalized Z^5-hypersurface ϕ,ψ surface of Ala^{23} in apokedarcidin. The chemical shifts of Ala^{23} are $N = 122.0$, $H^N = 9.2$, $C^\alpha = 49.2$, $H^\alpha = 5.62$, and $C^\beta = 21.9$. When dihedral restraints of $\phi = -120° \pm 40°$ and $\psi = 120° \pm 40°$ are used, the Z^5-hypersurface volume enclosed by these restraints is 0.69. (Right) Normalized Z^5-hypersurface ϕ,ψ surface of Val^{63} in human macrophage inhibitory protein. The chemical shifts of Val^{63} are $N = 119.0$, $H^N = 8.2$, $C^\alpha = 67.2$, $H^\alpha = 3.12$, and $C^\beta = 31.7$. When dihedral restraints of $\phi = -60° \pm 40°$ and $\psi = -40° \pm 40°$ are used, the Z^5-hypersurface volume enclosed by these restraints is 0.86.

downfield C^α chemical shifts are associated with α-structural features and upfield chemical shifts with β-structural features. For H^α, the most downfield shifts are associated with β and the more upfield with α.

The correlations of the C^β and carbonyl carbon sites are shown in Fig. 3. The pattern for the carbonyl carbons correlates with structure more so than that of the C^β sites. Thus, the chemical shifts of the carbonyl carbons may be more useful for ϕ and ψ determination than those of the C^β sites which also have significant dependence on χ_1. All six sets of maps correlating chemical shift with ϕ and ψ dihedral angles have the same shape since all six are based on the same set of dihedral angles observed for the 49 proteins.

A Z-surface approach was used to empirically correlate chemical shifts with the most likely backbone dihedral angles. A similar approach was previously proposed for correlating predicted and experimental dihedral angles (Le et al., 1995). The probability, Z, that a particular chemical shift corresponds to a particular dihedral angle is $\exp(-(\delta - \delta(\phi,\psi))^2)/W)$, which is unitless. In this equation, δ is the experimental chemical shift, $\delta(\phi,\psi)$ is the chemical shift template as a function of the ϕ and ψ dihedral angles for a particular amino acid, and W is twice the expected mean-square deviation between the experimental and the statistical evaluation of chemical shifts.

The multidimensional hypersurfaces were made by multiplying together the individual Z-surfaces of the different atoms in an amino acid. The Z^5-hypersurface utilizes the amide ^{15}N, $^{13}C^\alpha$, $^{13}C^\beta$, amide proton and α-proton chemical shifts to define the backbone conformations that have the highest probability of being consistent with *all of the backbone chemical shifts of the particular amino acid*. This approach has the advantage of utilizing all or any combination of the experimental chemical shift information simultaneously with individual weighting to exploit all the correlations between the chemical shifts.

Since the information in the chemical shifts of the distinct sites is not independent, the gain for the simultaneous use of all the chemical shifts is not optimal. For example, the ^{13}C chemical shift of the β-position appears to offer information that is largely, though not entirely, redundant to that of the α-position (Luginbühl et al., 1995). The level of independence of the chemical shifts of the distinct sites cannot be fully assessed until more information is available.

The mean-square deviations were determined for the chemical shift templates based on 14 amino acids as well as for the chemical shifts of leucine at the idealized α-helix and β-sheet regions. Leucine was used for this since it is the amino acid for which there is the most information. The determined values for twice the mean-square deviations are 13.5 for W^N, 10.0 for W^{C^α}, 12.5 for W^{C^β}, 0.6 for W^{H^N} and 0.5 for W^{H^α} for leucine. These mean-

square deviations correspond very well with the values obtained previously (Spera and Bax, 1991) for $^{13}C^{\alpha}$ and $^{13}C^{\beta}$. The mean-square deviation of the template, which is based on 14 amino acids, is about an order of magnitude larger for each site. The average of the mean-square deviations of leucine and that of the template, used in our calculations as the template deviation, may overstate the variation due to differences between the amino acids whereas the variation in the leucine data set may understate the expected variation.

Bins where the Z^5-hypersurface and the $Z^N Z^{C^{\alpha}} Z^{C^{\beta}}$-hypersurface probabilities were greater than 0.03 were used to define a rectangle in dihedral space of the ϕ,ψ surface and used as the chemical shift dihedral angle restraints. That is, the dihedral was constrained to the rectangle consistent with all the chemical shifts. Restraints were applied when the normalized volume resulting from the dihedral constraints was greater than 0.65 for an α-helical restraint and greater than 0.6 for any other dihedral angle restraints. Dihedral angle restraints were not allowed to become tighter than $\pm 40°$ and were allowed to be as large as $\pm 80°$. Typical, initial α-helical dihedral restraints were $\phi = -70° \pm 50°$ and $\psi = -30° \pm 50°$ and $\phi = -110° \pm 50°$ and $\psi = 130° \pm 70°$ for β-regions.

This normalized hypersurface approach allows identification of the dihedral angles of highest probability and allows weighting of all amino acids equally. These features and the use of a probability threshold score to define a chemical shift dihedral angle hypersurface restraint make the normalized hypersurface approach very appealing. The Z^5-normalized surfaces for Ala^{23} of apokedarcidin and Val^{63} of human macrophage protein are shown in Fig. 4.

Human macrophage inhibitory protein (Garrett et al., 1994; Lodi et al., 1994), apokedarcidin (Constantine et al., 1994), villin 14T (Markus et al., 1994; G. Wagner (1996) personal communication) and profilin (Metzler et al., 1993) were chosen as test proteins since these are four of the largest systems for which the necessary structural and NMR information was available. The NMR information used to solve the structures of human macrophage inhibitory protein and profilin was obtained from the Protein Databank. The NMR information used to solve the structures of apokedarcidin and villin 14T was obtained from the authors. All the structures were calculated using the same NOE and hydrogen bond information that was used for the determination of the reference PDB structure. The structures were calculated here using simulated annealing and structure refinement protocols along with the chemical shift Z^5-hypersurfaces as restraints as test cases of the methodology. This normalized hypersurface approach allows identification of the dihedral angle regions of highest probability and also allows weighting of any combination of chemical shifts individually.

The Z^5-hypersurfaces for profilin were also calculated using chemical shift templates with and without the profilin structure and chemical shifts in the template. The root-mean-square deviations (rmsd values) between all the bins of the 14 amino acid template with and without the profilin chemical shifts were 0.079 for ^{15}N, 0.002 for $^{1}H^{N}$, 0.042 for $^{13}C^{\alpha}$, 0.0006 for $^{1}H^{\alpha}$, and 0.157 for $^{13}C^{\beta}$. The rmsd values between all the bins of the 14 amino acid template with and without the villin 14T chemical shifts were 0.030 for ^{15}N, 0.001 for $^{1}H^{N}$, 0.046 for $^{13}C^{\alpha}$, 0.0005 for $^{1}H^{\alpha}$, and 0.089 for $^{13}C^{\beta}$. The rmsd values between the 14 amino acid template with and without the profilin or villin 14T chemical shifts were very small when compared to the mean-square deviations used to determine the Z-score probabilities. The summed, normalized Z-scores of the dihedral restraints in profilin and villin 14T did not vary by more than 0.01 due to the inclusion of that protein's information into the database. As these deviations are statistically insignificant, it appears that the inclusion of a specific protein's information does not bias the database.

The simulated annealing protocol, defined below, with no NOEs and no dihedral angle restraints was used to form a totally denatured starting structure using the PDB structure as the beginning structure. This denatured structure was visually checked to confirm its denatured and thermally random configuration before submitting it to simulated annealing. The resulting structure with the lowest energy had its ϕ and ψ dihedral angles determined and was then used in structure determination protocol. The Z^5-hypersurface volumes enclosed by the dihedral constraints were reduced from 0.65 to 0.55 for α-helical dihedral restraints and from 0.6 to 0.5 for all the other dihedral angle restraints. This allowed all dihedral restraints to be reduced to an uncertainty of ± 40 or $50°$. Typical α-helical dihedral restraints were $\phi = -60° \pm 40°$ and $\psi = -40° \pm 40°$ and β-sheet dihedral restraints were $\phi = -120° \pm 40°$ and $\psi = 130° \pm 50°$.

Typically, the number of dihedral constraints increased by 2–15% at this stage. This increase arises since some amino acids had bins with normalized Z^5-scores greater than 0.03 that conformed to a region with strong statistical Z-scores not within the annealed structure. At this stage, the ϕ and ψ dihedral angles of the lowest energy annealed structure were determined. If the dihedral angles of an unconstrained amino acid in the annealed structure were in a region of sufficiently high probability, greater than 0.55 for α-helices or 0.50 for all β-sheets, then the dihedral restraints were added during the structure refinement protocol. There were no structure calculations where positive ϕ angle restraints were used because the volume of the normalized, enclosed probability around the left-handed helix region was never greater than 0.50. There were cases where the probability in the left-handed region was greater than 0.03.

All structure calculations were performed with the use of X-PLOR 3.1 (Le and Oldfield, 1994) on an IBM 3CT.

The simulated annealing (Nilges et al., 1988) protocols started with 500 steps of energy minimization, followed by 4000 steps at 2 fs per time step, 8 ps total, of molecular dynamics at 1000 K with a scaled energy function such that angular force constants were multiplied by 0.4, torsions were multiplied by 0.1, and van der Waals terms were multiplied by 0.002. This was followed by another 2000 steps at 3 fs per time step, 6 ps total, of molecular dynamics at 1000 K with an intact energy function, except for the van der Waals which was scaled to 0.002 its normal value. The system was then cooled by dropping the temperature in 50 K intervals to a final temperature of 200 K. At each temperature, 625 steps at 3 fs per time step, 1.875 ps total, of molecular dynamics was carried out while scaling the van der Waals radii down to 0.75, with the normal van der Waals radii used at 200 K. This was followed by 2000 steps Powell conjugate energy minimization with the van der Waals energy function multiplied by 4.0. After the simulated annealing to 100 K, 500 steps of energy minimization with a van der Waals energy function multiplied by 4.0 was then executed followed by 100 steps of energy minimization with a scale factor of 200 for both NOE and dihedral angle constraints. Of the 10 calculated structures, the one structure with the lowest total energy and fewest violations was saved for use in refined simulated annealing.

Refined simulated annealing consisted of molecular dynamics first at 1000 K and then at lower temperatures. The temperature was lowered in 50 K increments to 100 K. At each temperature, 416 steps at 2 fs per time step, 0.84 ps total, of molecular dynamics was carried out. A hard square potential was used for the NOE restraints and a biharmonic potential was used for the dihedral angle restraints. The 10 lowest energy structures, out of a total of 20, with no NOE violations over 0.4 Å and no dihedral angle violations over 5° were saved and used to produce a final, averaged refined structure.

The evaluation of the normalized Z^5-hypersurface of apokedarcidin gave 16 ϕ and one ψ individual dihedral angle restraints and both ϕ and ψ for 54 residues for a total of 125 dihedral angle restraints during the refined structure determination. All 125 of these restraints along with the amide–amide NOEs were used to obtain the structure shown in Fig. 5. The first three amino acids are not shown since amide–amide NOE information was not available for these residues. The structure determined using only amide to amide NOEs and no dihedral restraints had a lower precision and lower accuracy to the PDB coordinates than the structure determined with no dihedral restraints. The family of structures determined with dihedral restraints is more tightly grouped than the structure determined with no dihedral restraints. The structure calculation results for apokedarcidin are summarized in Table 3.

The evaluation of the normalized Z^5-hypersurface for all 114 amino acids of villin 14T gave 26 ϕ and two ψ individual dihedral angle restraints and both ϕ and ψ for 64 residues for a total of 156 dihedral angle restraints. The evaluation of the normalized Z^5-hypersurface for all 133 amino acids of profilin gave 19 ϕ and one ψ individual dihedral angle restraints and both ϕ and ψ for 76 residues for a total of 172 dihedral angle restraints. The evaluation of the normalized Z^5-hypersurface of human macrophage inhibitory protein gave 11 ϕ and no ψ individual dihedral angle restraints and both ϕ and ψ for 38 residues of each monomer for a total of 174 dihedral angle restraints in each dimer. All 174 of these restraints were used along with the amide–amide NOEs to obtain a structure.

The only positions where the Z-score hypersurface calculations produced a dihedral restraint that was significantly different from the PDB structure were found in turns for both the apokedarcidin and profilin structures. Asp^{15} in apokedarcidin had an α-helical ϕ restraint during its original structure calculation and ended up in the β-sheet region with a ϕ angle of $-67.2°$, and a ψ dihedral angle of 130.6°. The Z^5 calculations showed that Asp^{15} of apokedarcidin was an α-helical residue. In all the calcula-

TABLE 3
NUMBER OF NOE AND DIHEDRAL ANGLE CONSTRAINTS USED DURING STRUCTURE DETERMINATION, THE BACKBONE RMSD PRECISION FOR THE FAMILY OF 10 STRUCTURES TO THEIR MEAN STRUCTURE, AND THE BACKBONE RMSD ACCURACY OF THE MEAN STRUCTURE TO THE PDB STRUCTURE FOR APOKEDARCIDIN

Parameter	akp 4–114	akpno 4–114	akp VT	akp VTFS	akpno VTFS	akp PDB
Number of NOEs	70	70	253	334	334	765
Number of chemical shift restraints	125	0	125	125	0	0
Number of J-coupling restraints	0	0	0	0	0	112
Backbone rmsd precision (Å)	3.67	3.87	2.18	2.51	2.42	0.68
Backbone rmsd accuracy (Å)	5.37	6.44	4.05	4.19	4.44	

akp 4–114: structure calculation of amino acids 4 through 114 using only amide to amide NOEs and chemical shift determined dihedral restraints; akpno 4–114: structure calculation of amino acids 4 through 114 using only amide to amide NOEs and no dihedral restraints; akp VT: structure calculation using amide to amide, amide to V and T residue proton and V and T proton to V and T proton NOEs and chemical shift determined dihedral restraints; akp VTFS: structure calculation using amide to amide, amide to V, T, F, and S proton and V, T, F, and S proton to V, T, F, and S proton NOEs and chemical shift determined dihedral restraints; akpno VTFS: structure calculation using amide to amide, amide to V, T, F, and S proton and V, T, F, and S proton to V, T, F, and S proton NOEs and no chemical shift determined dihedral restraints; akp PDB: structure calculation for the PDB structure.

TABLE 4
STRUCTURE CALCULATION RESULTS FOR VILLIN 14T

Parameter	vil 19–99	vilno 19–99	vil VY	vil VYFK	vilno VYFK	vil PDB
Number of NOEs	75	75	161	227	227	765
Number of chemical shift restraints	156	0	156	156	0	0
Number of J-coupling restraints	0	0	0	0	0	113
Backbone rmsd precision (Å)	4.40	4.55	3.55	2.54	2.75	1.15
Backbone rmsd accuracy (Å)	9.79	11.66	7.55	5.06	10.62	

vil 19–99: structure calculation of amino acids 19 through 99 using only amide to amide NOEs and chemical shift determined dihedral restraints; vilno 19–99: structure calculation of amino acids 19 through 99 using only amide to amide NOEs and no dihedral restraints; vil VY: structure calculation using amide to amide, amide to V and Y residue proton and V and Y proton to V and Y proton NOEs and chemical shift determined dihedral restraints; vil VYFK: structure calculation using amide to amide, amide to V, Y, F, and K proton and V, Y, F, and K proton to V, Y, F, and K proton NOEs and chemical shift determined dihedral restraints; vilno VYFK: structure calculation using amide to amide, amide to V, Y, F, and K proton and V, Y, F, and K proton to V, Y, F, and K proton NOEs and no chemical shift determined dihedral restraints; vil PDB: structure calculation for the pdb structure.

tions, the residue ended up with α-helical ϕ and ψ dihedral angles with no NOE violations greater than 0.4 Å or dihedral restraint violations greater than 5°. The normalized Z-score for this residue was 0.65.

Asp^{54} in apokedarcidin was in a left-handed helix configuration during the original PDB structure calculation. In this original PDB structure calculation, Asp^{54} had no dihedral restraints and very few NOEs and the Z^5-hypersurface had a strong α-helical appearance. The α-helical dihedral angle restraints for Asp^{54} in apokedarcidin slightly changed the overall folding pattern for apokedarcidin during the calculations and this may be the reason why the overall backbone rmsd was not lower than 4.0 Å.

For profilin, Ser^{75} and Lys^{115} had Z-hypersurface restraints that were different from the dihedral angles of the PDB structure. While Ser^{75} had a β-sheet type ϕ dihedral constraint, it ended up in a 3_{10} helix conformation. Lys^{115} had one of only five β-sheet ψ dihedral angle restraints during PDB structure calculation. Z^5-hypersurface calculations showed a strong correlation to a 3_{10}-helix configuration. All four residues that exhibited a disparity between the Z^5-hypersurface dihedral angle restraint and the PDB dihedral angle were in turn configurations. It appears that, in these cases, there was insufficient NOE information to refine the conformations of all the turn regions.

All the chemical shift template and probability plots were generated using EXCEL. A smoothing function was used at the edges of bins with probability density to bins where there was no probability. The bins with no probability are not on the template surface. Thus, smoothing occurred from the bins where $-180 < \psi < -160$ to bins where $-160 < \psi < -140$, but there was no smoothing from the bottom, $-180 < \psi < -160$, of the graph to the top of the graphs, $160 < \psi < 180$.

Results and Discussion

An advantage of simultaneous correlation of all the chemical shifts is illustrated by the correlation map for Ala^{23} of apokedarcidin in Fig. 4. The region of the ϕ and ψ dihedral angle map with the highest correlation to the five experimental chemical shifts is in the β-region. The correlation map for Val^{63} of human macrophage inhibitory protein has the region of the ϕ and ψ dihedral angle map with the highest correlation in the α-region. These are typical maps, with one chosen for being in the α-region and one in the β-region. It is seen that the Z^5 correlation maps define regions that are consistent with the five experimental chemical shifts.

A series of structure calculations were carried out and

TABLE 5
STRUCTURE CALCULATION RESULTS FOR PROFILIN

Parameter	pfl 18–114	pflno 18–114	pfl LT	pfl LTDY	pflno LTDY	pfl PDB
Number of NOEs and hydrogen bonds	306	306	501	599	599	1813
Number of chemical shift restraints	172	0	172	172	0	0
Number of J-coupling restraints	0	0	0	0	0	199
Backbone rmsd precision (Å)	3.84	3.96	1.22	1.14	1.85	0.58
Backbone rmsd accuracy (Å)	14.35	14.05	3.44	3.52	6.59	

pfl 18–114: structure calculation of amino acids 18 through 114 using only amide to amide NOEs and chemical shift determined dihedral restraints. pflno 18–114: structure calculation of amino acids 18 through 114 using only amide to amide NOEs and no dihedral restraints; pfl LT: structure calculation using amide to amide, amide to L and T residue proton and L and T proton to L and T proton NOEs and chemical shift determined dihedral restraints; pfl LTDY: structure calculation using amide to amide, amide to L, T, D, and Y proton and L, T, D, and Y proton to L, T, D, and Y proton NOEs and chemical shift determined dihedral restraints; pflno LTDY: structure calculation using amide to amide, amide to L, T, D, and Y proton and L, T, D, and Y proton to L, T, D, and Y proton NOEs and no chemical shift determined dihedral restraints; pfl PDB: structure calculation for the PDB structure.

TABLE 6
STRUCTURE CALCULATION RESULTS FOR HUMAN MACROPHAGE INHIBITORY PROTEIN

Parameter	hum 6–52	humno 6–52	hum SV	hum SVFD	humno SVFD	hum PDB
Number of NOEs and hydrogen bonds	460	460	748	1040	1040	3366
Number of chemical shift restraints	174	0	174	174	0	0
Number of J-coupling restraints	0	0	0	0	0	220
Backbone rmsd precision (Å)	2.87	4.33	3.12	2.49	3.58	0.30
Backbone rmsd accuracy (Å)	6.19	9.48	8.50	3.14	7.09	

hum 6–52: structure calculation of amino acids 6 through 52 using only amide to amide NOEs and chemical shift determined dihedral restraints; humno: structure calculation using only amide to amide NOEs and no dihedral restraints; hum SV: structure calculation using amide to amide, amide to S and V residue proton and S and V proton to S and V proton NOEs and chemical shift determined dihedral restraints; hum SVFD: structure calculation using amide to amide, amide to S, V, F, and D proton and S, V, F, and D proton to S, V, F, and D proton NOEs and chemical shift determined dihedral restraints; humno SFVFD: structure calculation using amide to amide, amide to S, V, F, and D proton and S, V, F, and D proton to S, V, F, and D proton NOEs and no chemical shift determined dihedral restraints; hum PDB: structure calculation for the PDB structure.

the results are listed in Tables 4, 5, and 6 for villin 14T, profilin, and human macrophage inhibitory protein, respectively. Structures were calculated with and without the inclusion of the chemical shift based restraints. The analysis of the structures showed that the inclusion of the chemical shift determined dihedral restraint structures typically increases the accuracy and precision of the backbone atoms. The structures determined using only the information in the amide–amide NOEs have relatively large rmsd values to the PDB structures and the inclusion of the chemical shift restraints improves the quality of the structures in each case. For profilin, there is not enough amide–amide NOE information available to allow the determination of the tertiary fold of profilin. The apokedarcidin structure determined by this approach is shown in Fig. 5.

The structures obtained using only the amide–amide NOE and chemical shift restraints are not highly defined, so additional structure calculations were carried out using the data that could be obtained on proteins with just a few protonated amino acids. There were at least two structures (Grzesiek et al., 1992; Shan et al., 1996) that were determined based on the use of selectively protonated methyl groups in an otherwise deuterated protein. Methyl and amino protons correspond to about 30% of the protons in a typical protein. The partial deuteration of four different amino acids may lead to less spectral overlap than that observed with the selective protonation of methyl groups. Part of the trade-off is that the range of chemical shifts of the amino acids will typically be wide compared to that of the methyls while the methyls will typically have smaller line widths. The choice of which residues should be selectively deuterated can also be based on information about an active site or drug binding site. For illustration purposes, the amino acids with the highest frequency were used here, with a bias towards aromatic and aliphatic amino acids.

The structure of human macrophage inhibitory protein was determined using the NOE data that could be obtained with selectively deuterated proteins. One data set, SV, included the amide proton NOEs as well as the NOEs between serine and valine residues in addition to the chemical shift and amide–amide NOEs. A second data set, SVFD, included the amide proton NOEs of serine, valine, phenylalanine, and aspartic acid as well as the proton–proton NOEs between these residues in addition to the chemical shift and amide–amide NOE information. The results in Table 6 indicate that the addition of the chemical shift restraints more than halves the rmsd of the SVFD structure to the PDB structure, and the structures are shown in Fig. 6. Similar drops are obtained for the structures of villin and profilin when the NOE data on the four protonated amino acid protein are combined with the chemical shift restraints. A comparable drop is not observed for apokedarcidin since the backbone rmsd without the inclusion of the chemical shift restraints is comparably much better than for the other three proteins.

The results indicate that for all four proteins, which were essentially randomly selected, reasonable resolution structures can be obtained with a relatively small data set. Fairly good structures could be obtained in each case with the use of the NOE data on samples that contain four protonated amino acids, the amide NOEs and the chemical shift restraints.

Analogous results have been obtained for apokedarcidin, villin 14T, and profilin, with the precision and accuracy values given in Tables 3, 4, and 5. For apokedarcidin, the effects of protonating only residues VT (valine and threonine) or VTFS (valine, threonine, phenylalanine and serine) were simulated. For villin 14T, the effects of protonating only residues VY (valine and tyrosine) or VYFK (valine, tyrosine, phenylalanine, and lysine) were simulated. For profilin, the effects of protonating only residues LT (leucine and threonine) or LTDY (leucine, threonine, aspartic acid and tyrosine) were simulated. In each case, the accuracy of the four amino acid protonated structure and the PDB structure is small enough to indicate that the overall tertiary fold of the protein has been determined.

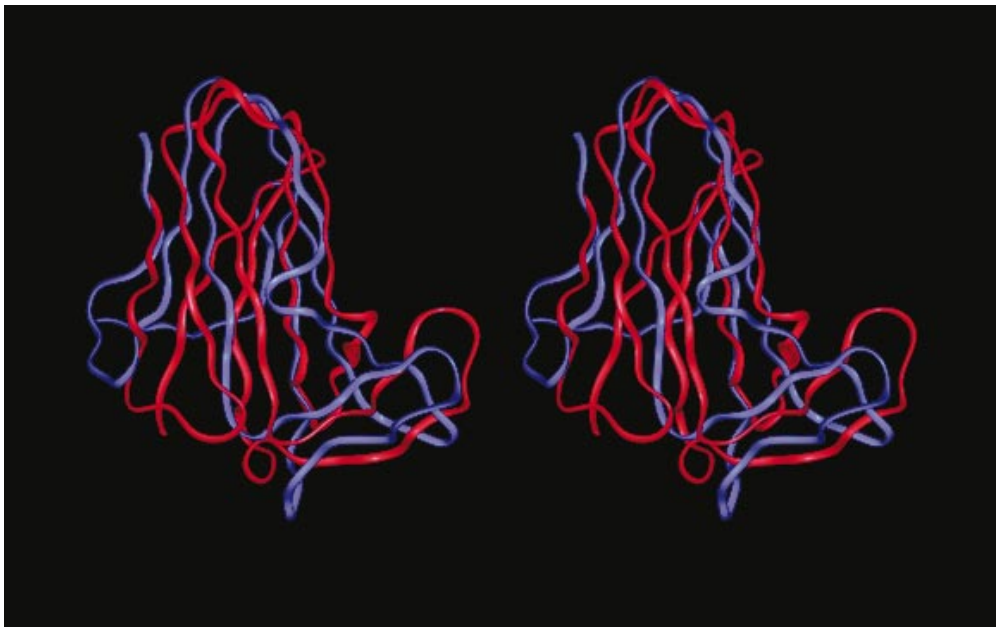

Fig. 5. The stereoview of the truncated structures of apokedarcidin determined using conventional NMR methods is shown in red and the averaged refined structure determined from chemical shifts and from simulating the effects of deuterating all amino acids is shown in blue. At the bottom the front and back view of the truncated structures of human macrophage protein determined using conventional NMR methods is shown in red and the averaged refined structure determined from chemical shifts and from simulating the effects of deuterating all amino acids is shown in blue.

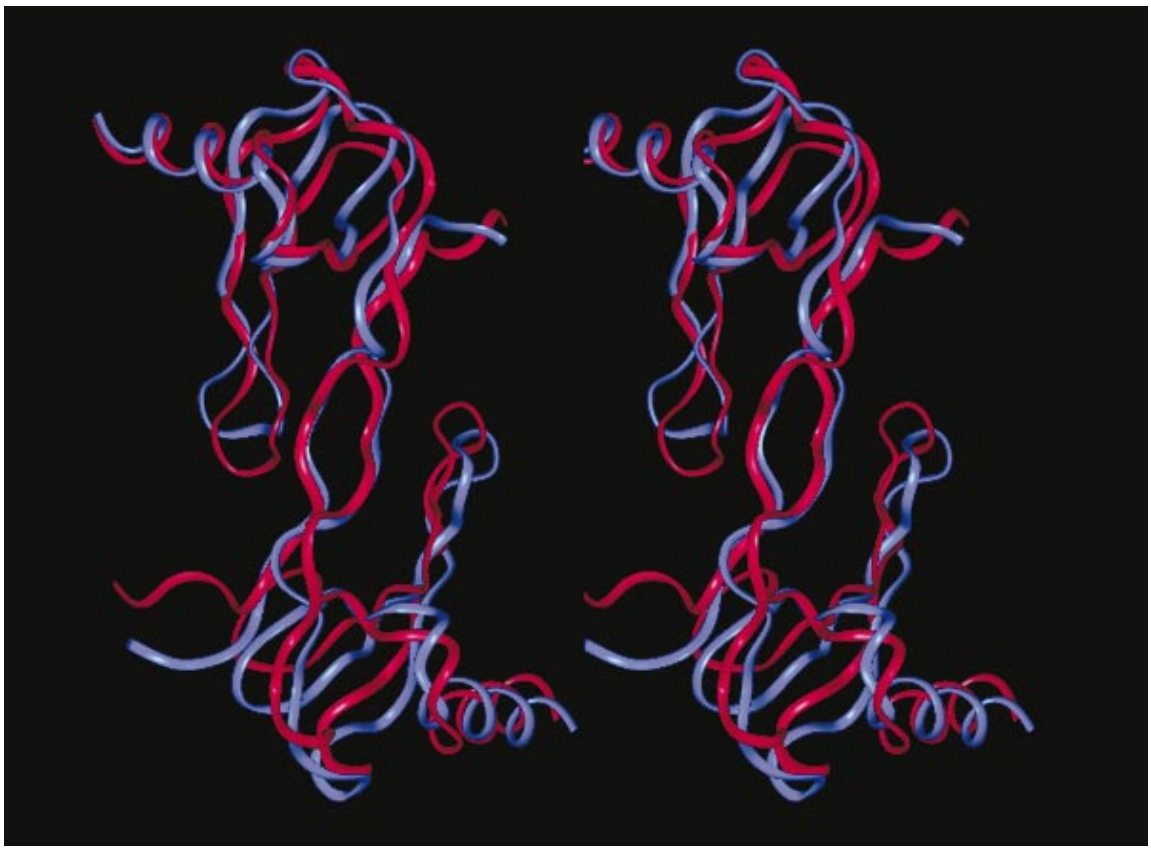

Fig. 6. The stereoview of the structures of human macrophage inhibitory protein determined using conventional NMR methods is shown in red and the averaged refined structure determined from chemical shifts and from simulating the effects of deuterating all the amino acids, except for the serine, valine, proline, and aspartic acid residues (30% of all the amino acids protonated and 30% of all the NOE and hydrogen bond constraints used), is shown in blue.

These results indicate that the structures are reasonably well defined using a modest-sized NOE set along with chemical shift based dihedral angle restraints. The results on these four proteins indicate that the combined use of the chemical shifts of the backbone atoms, the amide–amide NOEs and the NOEs of a small number of residue types can allow the overall structure of a protein to be determined. The NOEs of a few amino acid types can be obtained simultaneously using proteins with only a few protonated residues.

This empirical approach has several advantages and disadvantages over current approaches. One disadvantage of this approach is that unusual structural features and their associated chemical shifts will not be in the database. Attempting to fit a feature not present in the data base should be identifiable by its large energy terms. An advantage is that dihedral restraints are easily incorporated into structure determination procedures on proteins of all sizes. The incorporation of the chemical shift based restraints can significantly enhance the quality of the structures determined as well as limit the amount of information needed to obtain a structure. The chemical shifts are determined as part of the assignment process and including them into the structure determination does not require, in general, additional experiments.

One effect that has not been included here are the effects of ring current shifts on the chemical shifts. Procedures for calculating ring current effects from protein structures have been developed. Ring current shifts can be added into future protocols to aid the refinement process.

The approach outlined here may allow the global fold of relatively large proteins and protein complexes to be determined using NMR information that can be obtained by currently available means. The global folds determined with the most limited data sets can be of sufficient resolution to obtain the basic structural features. The chemical shift correlations will become more precise as the database size increases and the methodology will be developed further. Some of the refinement to this procedure may include the use of carbonyl chemical shifts in the Z^N-hypersurface calculations, nearest-neighbor effects, tightening of the dihedral restraints, and using more than one template for each chemical shift. This approach can also be added to the current methods to refine protein structures and is being used on complexes of uracil glycosylase with uracil glycosylase inhibitor. The results suggest that structure determination based on chemical shifts determined via solid-state NMR methods along with limited long-range distance information, determined from dephasing experiments, may be feasible.

Acknowledgements

The research at Wesleyan was supported, in part, by Grant GM-51298 from the National Institutes of Health.

References

Abeygunawardana, C., Weber, D.J., Frick, D.N., Bessman, M.J. and Mildvan, A.S. (1993) *Biochemistry*, **32**, 13071–13080.

Abeygunawardana, C., Weber, D.J., Gittis, A.G., Frick, D.N., Lin, J., Miller, A.-F., Bessman, M.J. and Mildvan, A.S. (1995) *Biochemistry*, **34**, 14997–15005.

Ames, J.A., Tanaka, T., Styer, L. and Ikura, M. (1994) *Biochemistry*, **33**, 10743–10753.

Archer, S.J., Bax, A., Roberts, A.B., Sporn, M.B., Ogawa, Y., Piez, K.A., Weatherbee, J.A., Tsang, M.L.-S., Lucas, R., Zheng, B.-L., Wenker, J. and Torchia, D.A. (1993) *Biochemistry*, **32**, 1152–1163.

Bagby, S., Harvey, T.S., Eagle, S.G., Inouye, S. and Ikura, M. (1994a) *Structure*, **2**, 107–122.

Bagby, S., Harvey, T.S., Kay, L.E., Eagle, S.G., Inouye, S. and Ikura, M. (1994b) *Biochemistry*, **33**, 2409–2421.

Balasubramanian, S., Beger, R.D., Bennett, S.E., Mosbaugh, D.W. and Bolton, P.H. (1995) *J. Biol. Chem.*, **270**, 296–303.

Banci, L., Bertini, I., Eltis, L.D., Felli, I., Kastrau, D.H.W., Luchina, C., Piccioli, M., Paerattelli, R. and Smith, M. (1994) *Eur. J. Biochem.*, **225**, 715–725.

Baumann, H., Paulsen, K., Kovacs, H., Berglund, H., Wright, A.P.H., Gustafsson, J.-A. and Hard, T. (1993) *Biochemistry*, **32**, 13463–13471.

Beger, R.D., Balasubramanian, S., Bennett, S., Mosbaugh, D.W. and Bolton, P.H. (1995) *J. Biol. Chem.*, **270**, 16840–16847.

Berglund, H., Kovacs, H., Wright, K.-D., Gustafsson, J.-A. and Hard, T. (1992) *Biochemistry*, **31**, 12001–12011.

Bertini, I., Felli, I.C., Kastrau, D.H.W., Luchinat, C., Piccioli, M. and Viezzoli, M.S. (1994) *Eur. J. Biochem.*, **225**, 703–714.

Borden, K.L.B., Bauer, C.J., Frenkiel, T.A., Beckman, P. and Lane, A.N. (1992) *Eur. J. Biochem.*, **204**, 137–146.

Cerf, C., Lippens, G., Ramakrishnan, V., Muyldermans, S., Segers, A., Wyns, L., Wodak, J. and Hallenga, K. (1994) *Biochemistry*, **33**, 11079–11086.

Clayden, N.J. and Williams, R.J.P. (1982) *J. Magn. Reson.*, **49**, 383–395.

Clore, G.M., Wingfield, P.T. and Gronenborn, A.M. (1991) *Biochemistry*, **30**, 2315–2323.

Clore, G.M., Bax, A., Omichinski, J.G. and Gronenborn, A.M. (1994) *Nat. Struct. Biol.*, **2**, 89–94.

Clore, G.M., Omichinski, J.G., Sakaguicki, K., Zambrano, N., Sakamoto, H., Appella, E. and Gronenborn, A.M. (1995) *Nat. Struct. Biol.*, **2**, 321–333.

Clubb, R.T., Thanabal, V., Fejzo, J., Ferguson, S.B., Zydowsky, L., Baker, C.H., Walsh, C.T. and Wagner, G. (1993) *Biochemistry*, **37**, 6391–6401.

Clubb, R.T., Ferguson, S.B., Walsh, C.T. and Wagner, G. (1994) *Biochemistry*, **33**, 2761–2772.

Constantine, K.L., Goldfarb, V., Wittekind, M., Anthony, J., Ng, S.-C. and Mueller, L. (1992) *Biochemistry*, **31**, 5033–5043.

Constantine, K.L., Goldfarb, V., Wittekind, M., Friedrichs, M.S., Anthony, J., Ng, S.-C. and Mueller, L. (1993) *J. Biomol. NMR*, **3**, 41–54.

Constantine, K.L., Colson, K.L., Wittekind, M., Friedrichs, M.S., Zein, N., Tuttle, J., Langley, D.R., Leet, J.E., Schroeder, D.R., Lam, K.S., Farmer II, B.T., Metzler, W.J., Bruccoleri, R.E. and Mueller, L. (1994) *Biochemistry*, **33**, 11438–11452.

Cox, M., Van Tilborg, P.J.A., Laat, W.D., Boelens, R., Van Leeuwen, H.C., Van der Vliet, P.C. and Kaptein, R. (1993) *Biochemistry*, **32**, 6032–6040.

de Dios, A.C. and Oldfield, E. (1994) *J. Am. Chem. Soc.*, **116**, 5307–5314.

Donaldson, L.W., Petersen, J.M., Graves, B.J. and McIntosh, L.P. (1994) *Biochemistry*, **33**, 13509–13516.

Duyne, G.D.V., Standaert, R.F., Karplus, P.A., Schreiber, S.L. and Clardy, J. (1991) *Science*, **252**, 839–842.

Erikson, A.E., Cousens, L.S., Weaver, L.H. and Matthews, B.W. (1991) *Proc. Natl. Acad. Sci. USA*, **88**, 3441–3445.

Falzone, C.J., Kao, Y.-H., Zhao, J., Bryant, D.A. and Lecomte, J.T.J. (1994a) *Biochemistry*, **33**, 6052–6062.

Falzone, C.J., Kao, Y.-H., Zhao, J., MacLaughlin, K.L., Bryant, D.A. and Lecomte, J.T.J. (1994b) *Biochemistry*, **33**, 6043–6051.

Flaherty, K.M., Zozulya, S., Stryer, L. and McKay, D.B. (1993) *Cell*, **75**, 709–716.

Forman-Kay, J.D., Gronenborn, A.M., Kay, L.E., Wingfield, P.T. and Clore, G.M. (1990) *Biochemistry*, **29**, 1566–1572.

Forman-Kay, J.D., Clore, G.M., Wingfield, P.T. and Gronenborn, A.M. (1991) *Biochemistry*, **30**, 2685–2698.

Gardner, K.H., Rosen, M.K. and Kay, L.E. (1997) *Biochemistry*, **36**, 1389–1401.

Garrett, D.S., Lodi, P.J., Shamoo, Y., Williams, K.R., Clore, G.M. and Gronenborn, A.M. (1994) *Biochemistry*, **33**, 2852–2858.

Gooley, P.R., Johnson, B.A., Marcy, A.I., Cuca, G.C., Salowe, S.P., Hagmann, W.K., Esser, C.K. and Springer, J.P. (1993) *Biochemistry*, **32**, 13098–13108.

Gooley, P.R., O'Connel, J.F., Marcy, A.I., Cuca, G.C., Salowe, S.P., Bush, B.L., Hermes, J.D., Esser, C.K., Hagmann, W.K., Springer, J.P. and Johnson, B.A. (1994) *Nat. Struct. Biol.*, **1**, 111–118.

Gronenborn, A.M., Wingfield, P.T. and Clore, G.M. (1989) *Biochemistry*, **28**, 5081–5089.

Grzesiek, S., Dobeli, H., Gentz, R., Garotta, G., Labhardt, A.M. and Bax, A. (1992) *Biochemistry*, **31**, 8180–8190.

Hansen, A.P., Petros, A.M., Meadows, R.P., Nettesheim, D.G., Mazar, A.P., Olejniczak, E.T., Xu, R.X., Pederson, T.M., Hecklin, J. and Fesik, S.W. (1994) *Biochemistry*, **33**, 4847–4864.

Hynes, T.R. and Fox, R.O. (1991) *Proteins Struct. Funct. Genet.*, **10**, 92–105.

Ikura, M., Kay, L.E. and Bax, A. (1990) *Biochemistry*, **29**, 4659–4667.

Ikura, M., Clore, G.M., Gronenborn, A.M., Zhu, G., Klee, C.B. and Bax, A. (1992) *Science*, **256**, 632–638.

Jamin, N., Gabreilsen, O.S., Gilles, N., Lirsac, P.-N. and Toma, F. (1993) *Eur. J. Biochem.*, **216**, 147–154.

Kuszewski, J., Qin, J., Gronenborn, A.M. and Clore, G.M. (1995) *J. Magn. Reson.*, **B106**, 92–96.

Laws, D.D., Le, H., de Dios, A.C., Havlin, R.H. and Oldfield, E. (1995) *J. Am. Chem. Soc.*, **117**, 9542–9546.

Lawson, C.L., Zhang, R.G., Schevitz, R.W., Otwinowski, Z., Joachimiak, A. and Sigler, P.B. (1988) *Proteins*, **3**, 18–31.

Le, H. and Oldfield, E. (1994) *J. Biomol. NMR*, **4**, 341–348.

Le, H., Pearson, J.G., de Dios, A.C. and Oldfield, E. (1995) *J. Am. Chem. Soc.*, **117**, 3800–3807.

Lee, A.L., Kanaar, R., Rio, D.C. and Wemmer, D.E. (1994a) *Biochemistry*, **33**, 13775–13786.

Lee, W., T., S.H., Yin, Y., Tau, P., Litchfield, D. and Arrowsmith, C.H. (1994b) *Nat. Struct. Biol.*, **1**, 877–890.

Liang, H., Petros, A.M., Meadows, R.P., Yoon, H.S., Egan, D.A., Walter, K., Holzman, T.F., Robins, T. and Fesik, S.W. (1996) *Biochemistry*, **35**, 2095–2103.

Lodi, P.J., Garrett, D.S., Kuszewski, J., Tsang, M.L.S., Weatherbee, J.A., Leonard, W.J., Gronenborn, A.M. and Clore, G.M. (1994) *Science*, **263**, 1762–1767.

Loll, P.J. and Lattman, E.E. (1989) *Proteins Struct. Funct. Genet.*, **5**, 183–201.

Luginbühl, P., Szyperski, T. and Wüthrich, K. (1995) *J. Magn. Reson.*, **B109**, 229–233.

Markus, M.A., Nakayama, T., Matsudaira, P. and Wagner, G. (1994) *J. Biomol. NMR*, **4**, 553–574.

Matsuo, H., Shirakawa, M. and Kyogoku, Y. (1995) *J. Mol. Biol.*, **254**, 668–680.

McIntosh, L.P., Wand, A.J., Lowry, D.E., Redfield, A.G. and Dahlquist, F.W. (1990) *Biochemistry*, **29**, 6341–6362.

Metzler, W.J., Constantine, K.L., Friedrichs, M.S., Bell, A.J., Ernst, E.G., Lavoie, T. and Mueller, L. (1993) *Biochemistry*, **32**, 13818–13829.

Moy, F.J., Lowry, D.F., Matsumura, P., Dahlquist, F.W., Krywko, J.E. and Domaille, P.J. (1994) *Biochemistry*, **33**, 10731–10742.

Nilges, M., Clore, G.M. and Gronenborn, A.M. (1988) *FEBS Lett.*, **229**, 317–324.

Van Nuland, N.A.J., Van Dijk, A.A., Dijkstra, K., Van Hoesel, F.H.J., Scheek, R.M. and Robillard, G.T. (1992) *Eur. J. Biochem.*, **203**, 483–491.

Van Nuland, N.A.J., Scheek, R.M., Schaik, R.C.V. and Robillard, G.T. (1995) *J. Mol. Biol.*, **246**, 180–193.

Oh, B.H. and Markley, J.L. (1990) *Biochemistry*, **29**, 3993–4004.

Ösapay, K., Theriault, Y., Wright, P.E. and Case, D.A. (1994) *J. Mol. Biol.*, **244**, 183–197.

Pastore, A. and Saudek, V. (1990) *J. Magn. Reson.*, **83**, 165–176.

Pearson, J.G., Wang, J.-F., Markley, J.L., Le, H.-B. and Oldfield, E. (1995) *J. Am. Chem. Soc.*, **117**, 8823–8829.

Powers, R., Garrett, D.S., March, C.J., Frieden, E.A., Gronenborn, A.M. and Clore, G.M. (1992) *Biochemistry*, **31**, 4334–4346.

Powers, R., Garrett, D.S., March, C.J., Frieden, E.A., Gronenborn, A.M. and Clore, G.M. (1993) *Biochemistry*, **32**, 6744–6762.

Rose, D.R., Phipps, J., Michniewicz, J., Birnbaum, G.I., Ahmed, F.R., Muir, A., Anderson, W.F. and Narang, S.A. (1988) *Protein Eng.*, **2**, 277–283.

Rypniewski, W.R., Breiter, D.R., Benning, M.M., Wesenberg, G., Oh, B.H., Markley, J.L., Rayment, I. and Holden, H.M. (1991) *Biochemistry*, **30**, 4126–4131.

Schlunegger, M.P. and Gruetter, M.G. (1993) *J. Mol. Biol.*, **231**, 445–458.

Shan, X., Gardner, K.H., Muhandiram, D.R., Rao, N.S., Arrowsmith, C.H. and Kay, L.E. (1996) *J. Am. Chem. Soc.*, **118**, 6570–6579.

Skelton, N.J., Forsen, S. and Chazin, W.J. (1990) *Biochemistry*, **29**, 5752–5761.

Skelton, N.J., Akke, M., Kordel, J., Thulin, E., Forsen, S. and Chazin, W.J. (1992) *FEBS Lett.*, **303**, 136–140.

Spera, S. and Bax, A. (1991) *J. Am. Chem. Soc.*, **113**, 5490–5492.

Sternlicht, H. and Wilson, D. (1967) *Biochemistry*, **6**, 2881–2892.

Stockman, B.J., Scahill, T.A., Roy, M., Ulrich, E.L., Strakalatis, N.A., Brunner, D.P., Yem, A.W. and Jr., M.R.D. (1992) *Biochemistry*, **31**, 5237–5245.

Stockman, B.J., Scahill, T.A., Strakalatis, N.A., Brunner, D.P., Yem, A.W. and Jr., M.R.D. (1994) *FEBS Lett.*, **349**, 79–83.

Strzelecka, T.E., Hayes, J.J., Clore, G.M. and Gronenborn, A.M. (1995) *Biochemistry*, **34**, 2946–2955.

Szilágyi, L. and Jardetzky, O. (1989) *J. Magn. Reson.*, **83**, 441–449.

Theirault, Y., Pochapsky, T.C., Dalvit, C., Chiu, M.L., Sligar, S.G. and Wright, P.E. (1994) *J. Biomol. NMR*, **4**, 491–504.

Tigelaar, H.L. and Flygare, W.H. (1972) *J. Magn. Reson.*, **49**, 343–344.

Vincent, S.J.F., Zwahlen, C., Bolton, P.H., Logan, T.L. and Bodenhausen, G. (1996) *J. Am. Chem. Soc.*, **118**, 3531–3532.

Vinson, V.K., Archer, S.J., Lattman, E.E., Pollard, T.D. and Torchia, D.A. (1993) *J. Cell Biol.*, **122**, 1277–1283.

Vis, H., Boelens, R., Mariani, M., Stroop, R., Vorgias, C.E., Wilson, K.S. and Kaptein, R. (1994) *Biochemistry*, **33**, 14858–14870.

Vis, H., Mariani, M., Vorgias, C.E., Wilson, K.S., Kaptein, R. and Boelens, R. (1995) *J. Mol. Biol.*, **254**, 692–703.

Volkman, B.F., Nohaile, J.M., Amy, N.K., Kutsu, S. and Wemmer, D. (1995) *Biochemistry*, **34**, 1413–1424.

Vuister, G.W., Kim, S.-J., Wu, C. and Bax, A. (1994) *Biochemistry*, **33**, 10–16.

Wang, J., Hinck, A.P., Loh, S.N., LeMaster, D.M. and Markley, J.L. (1992) *Biochemistry*, **31**, 921–936.

Wishart, D.S., Sykes, B.D. and Richards, F.M. (1992) *Biochemistry*, **31**, 1647–1651.

Wishart, D.S. and Sykes, B.D. (1994) *J. Biomol. NMR*, **4**, 171–180.

Wüthrich, K. (1986) *NMR of Proteins and Nucleic Acids*, Wiley, New York, NY, U.S.A.

Xu, R.X., Nettesheim, D., Olejniczak, E.T., Meadows, R., Gemmecker, G. and Fesik, S.W. (1993) *Biopolymers*, **33**, 535–550.

Yu, L., Zhu, C.-X., Tse-Dinh, Y.-C. and Fesik, S.W. (1995) *Biochemistry*, **34**, 7622–7628.